J Nanostruct 16(1): 517-530, Winter 2026

RESEARCH PAPER

Factors Influencing the Enhanced Photocatalytic Degradation of Congo Red Dye Using SiO_2/ZnO Nanocomposite Under UV Irradiation

Alam Q. AL-Hussin, Hazim Yahya Al-gubury *, and Ali Taleb Bader

Department of Chemistry, College of Science for Women, University of Babylon, Hilla, Iraq

ARTICLE INFO

Article History:
Received 06 July 2025
Accepted 24 December 2025
Published 01 January 2026

Keywords:
Congo red dye
Degradation
Photo catalysis
SiO_2/ZnO nanocomposite
XRD

ABSTRACT

This study aims to evaluate the photocatalytic activity of a SiO_2/ZnO nanocomposite (where the surface characterized by using XRD , EDX and SEM techniques) for the degradation of organic pollutants, using Congo red dye as a model contaminant. Photocatalytic experiments were conducted using an aqueous solution containing 0.15 g of the nanocomposite per 100 mL of a 10 mg/L Congo red solution, under UV light irradiation. The influence of several operational parameters on the photocatalytic degradation efficiency was systematically investigated, including: Effect of catalyst dosage, a concentration of 0.15 g/100 mL was found to be effective, effect of initial dye concentration, various concentrations were tested, with 10 mg/L determined to be optimal, Effect of Initial pH of the solution, The photocatalytic performance was evaluated at different pH levels, with the best degradation observed at pH 8, Effect of addition of hydrogen peroxide (H_2O_2), the effect of H_2O_2 as an oxidizing agent was assessed to enhance the degradation efficiency, Effect of light intensity ,the effect of varying UV light intensity on the degradation process was examined and, Effect of reaction temperature, the influence of temperature on the photocatalytic reaction rate was analyzed. Kinetic and thermodynamic studies were carried out to understand the mechanism of degradation. The activation energy and other thermodynamic parameters were calculated using the Arrhenius and Eyring equations. The results were as follows: Activation Energy (Ea)= 38.61 kJ·mol^{-1},Enthalpy of Activation ($\Delta H°$) = 31.06 kJ·mol^{-1},Entropy of Activation ($\Delta S°$)= −0.14842 kJ·mol^{-1}·K^{-1}and Gibbs Free Energy of Activation ($\Delta G°$) = - 44.19 kJ·mol^{-1}.The degradation process was monitored using UV-Visible spectrophotometry to assess the concentration of the dye before and after irradiation.

How to cite this article
Q. AL-Hussin A., Y. Al-gubury H., Taleb Bader A. Factors Influencing the Enhanced Photocatalytic Degradation of Congo Red Dye Using SiO_2/ZnO Nanocomposite Under UV Irradiation. J Nanostruct, 2026; 16(1):517-530. DOI: 10.22052/JNS.2026.01.047

INTRODUCTION

In recent years, toxic organic pigments and their wastewater byproducts, generated from a wide range of industries including textiles, plastics, paper, pesticides, leather, and petrochemicals, have emerged as significant environmental pollutants, posing serious threats to aquatic ecosystems and human health. These hazardous dyes are major contributors to water pollution, with an estimated 10–15% of the dyes used in industrial processes discharged into wastewater streams. Due to their complex molecular

* *Corresponding Author Email: h.yahya40@yahoo.com*

structures and high chemical stability, the organic dyes present in industrial effluents are highly resistant to natural degradation processes [1]. To address this challenge, various physicochemical and biological treatment methods have been employed, such as chemical oxidation, adsorption, precipitation, ion exchange, biological treatment, reverse osmosis, and photocatalytic degradation. Synthetic dyes, which are chemically and physically robust, are widely used in textile manufacturing. Their high solubility and stability in water lead to persistent accumulation in industrial effluents, thereby posing long-term environmental and health hazards [2, 3].

In light of the growing concern over dye-contaminated water, photocatalytic degradation using semiconductor nanoparticles has recently garnered significant attention as a promising approach for the treatment and reclamation of polluted water bodies. This technique offers numerous advantages, including high efficiency, environmental safety, and the potential to degrade dyes without producing harmful intermediate byproducts in most cases. Under light irradiation at specific wavelengths, semiconductor nanoparticles are capable of generating electron–hole pairs that initiate a series of redox reactions. These reactions lead to the formation of hydroxyl radicals, which serve as the primary oxidizing species responsible for breaking down complex organic dye molecules into environmentally benign end-products [4, 5].

To mitigate the detrimental environmental impacts of these pollutants and comply with increasingly stringent environmental regulations, research on the treatment of azo dyes in wastewater has intensified in recent years. A range of conventional treatment methods encompassing physical, chemical, and biological approaches have been investigated for the effective removal of azo dyes from industrial effluents. The degradation of ecosystems due to human activities has become a critical global concern that demands serious attention. Among the most pressing environmental issues, water contamination stands out as a major contributor to ecosystem disruption. This pollution is primarily caused by a wide range of organic pollutants, leading to significant environmental and public health challenges worldwide. In particular, wastewater containing synthetic dyes discharged untreated from industries such as textiles, dyeing, pharmaceuticals, cosmetics, printing, and food processing poses a severe threat to freshwater resources and aquatic ecosystems [6, 7].

Nanocomposite coatings represent an emerging class of advanced surface treatments designed to offer intelligent, cost effective, and high performance solutions with exceptional functional properties. These coatings are increasingly employed in various applications, including corrosion resistance, antimicrobial activity, antifogging surfaces, and adhesive technologies. Compared to conventional coatings, nanocomposite coatings are often favored due to their enhanced structural morphology and the presence of phase-separated nanoscale domains, which contribute to superior performance characteristics. Typically, nanostructured filler particles are uniformly dispersed within a matrix to form a nanocomposite coating. Recently, the semiconductor nanomaterials have attracted a wide attention because of their exotic optical, electrical, electronic, photocatalytic, mechanical, thermal, etc. properties [8-10].

In recent years, semiconductor nanomaterials have garnered significant attention due to their unique and versatile properties, including optical, electrical, electronic, photocatalytic, mechanical, and thermal characteristics. Among these materials, photocatalytic semiconductors such as titanium dioxide (TiO_2) [11]and zinc oxide (ZnO) [12]have been widely studied for their potential applications in environmental remediation, particularly in water and air purification. In heterogeneous photo catalysis for water treatment, the degradation process typically involves four essential steps. Adsorption, of the pollutant molecules onto the surface of the photocatalyst. 2- Light absorption, by the photo catalyst, resulting in the excitation of electrons from the valence band (VB) to the conduction band (CB), creating electron–hole pairs; 3- Redox reactions, at the catalyst surface, where the photo generated charge carriers interact with adsorbed species (e.g., pollutants, water, or oxygen) to directly degrade contaminants or generate reactive oxygen species (ROS). 4- Desorption, of the reaction products from the catalyst surface. This sequence of processes enables the effective breakdown of organic pollutants into less harmful or mineralized products under light irradiation [13,14].

Congo red was first synthesized in 1883 by Paul Böttiger, an employee of the Friedrich

Bayer Company in Elberfeld, Germany. It is an organic azo dye with the chemical formula $C_{32}H_{22}N_6Na_2O_6S_2$, and is chemically identified as the sodium salt of 3,3'-((1,1'-biphenyl)-4,4'-diyl) bis(4-aminonaphthalene-1-sulfonic acid) as shown in Fig. 1. Congo red is water-soluble and forms a red colloidal solution; however, it exhibits higher solubility in organic solvents. Although historically used in the textile industry, the application of Congo red has been discontinued mainly due to its carcinogenic nature [15, 16].

MATERIALS AND METHODS

Chemicals

Fluka provided Congo red dye. Sodium hydroxide was provided by Fluka (Buchs, Switzerland), Hydrochloric acid was supplied by Fluka AG, Zinc oxide nanoparticles by Fluka AG, Silica oxide by Fluka AG, and Hydrogen peroxide by Fluka AG. All chemicals were employed without any further purification.

Photocatalytic degradation processes of Congo red dye using SiO_2/ZnO nanocomposite

SiO_2/ZnO nanocomposite surface was employed as a photocatalyst in degradation experiments aimed at breaking down Congo red dye in aqueous solution under ultraviolet (UV) light irradiation. The entire process was conducted in a custom-designed photoreactor consisting of two main components. The first component was equipped with a cooling system through which circulating water maintained a stable temperature of the suspension. The second component served as the reaction chamber, with a capacity of 100 mL, containing the dye suspension for photocatalytic degradation. A 100 mg/L stock solution of Congo red dye was prepared using distilled water. For each experimental run, 100 mL of the dye solution was mixed with 0.15 g of the SiO_2/ZnO nanocomposite. The mixture was stirred thoroughly to ensure homogeneous dispersion of the catalyst, forming a well-suspended solution. The prepared suspension was then irradiated with UV light. At regular intervals of 10 minutes, 2–3 mL aliquots were withdrawn from the reaction mixture using a syringe. The samples were immediately centrifuged at 3000 rpm for 10 minutes to separate the photocatalyst particles. The supernatant was then analyzed using a UV-Vis spectrophotometer to monitor changes in the dye's absorbance, allowing assessment of the photocatalytic degradation efficiency over time.

RESULTS AND DISCUSSION

Crystal structure and surface characterization

The XRD pattern exhibits a broad hump around 20–25° (2θ), characteristic of amorphous SiO_2 (Sánchez et al., 2009), together with sharp reflections attributable to hexagonal wurtzite ZnO (JCPDS 36-1451). The most intense ZnO peaks occur at approximately 31.8°, 34.4° and 36.2°, which correspond to the (100), (002), and (101) planes, respectively [17]. No secondary crystalline phases such as Zn_2SiO_4 or $Zn(OH)_2$ were detected within the instrument's sensitivity, indicating that ZnO is the only crystalline component and that SiO_2 remains amorphous after synthesis as shown

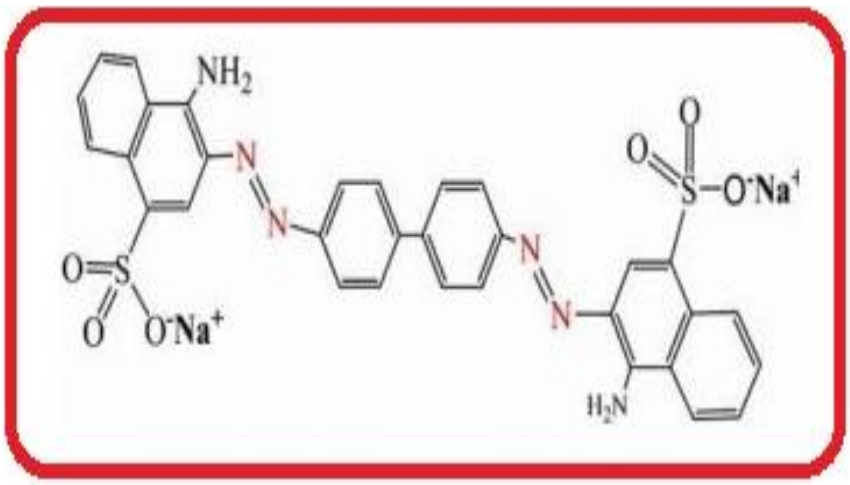

Fig. 1. Chemical structure of Congo red dye.

in Fig. 2a. Peak broadening relative to bulk ZnO suggests nanoscale crystallite size . The crystallite size can be calculated using the Scherrer equation.

The EDX spectrum reveals strong Si Kα and O Kα peaks, along with Zn Lα and Zn Kα lines, confirming the presence of Si, O, and Zn as the major elements [18]. The absence of foreign elements indicates high purity and effective removal of residual precursors during processing. While EDX provides only semi-quantitative data, due to the influence of the sampling depth and matrix effects, the results strongly support the successful incorporation of ZnO into the SiO_2 matrix without detectable contamination as shown in Fig. 2b.

The SEM micrographs at 1 µm (Fig. 2d) and 200 nm (Fig. 2c) scales display agglomerated spherical nanoparticles anchored to a rough SiO_2 substrate. At higher magnification, individual ZnO nanograins are visible, with estimated diameters in the tens of nanometers, in agreement with the XRD broadening. The aggregates exhibit cauliflower-like hierarchical structures, consistent with previous ZnO–SiO_2 composite studies. Such morphology provides a high surface area and strong interfacial contact between ZnO and the SiO_2 network, which can enhance photocatalytic or adsorption performance [19] as shown in Fig. 2c and d.

The combined XRD, EDX, and SEM results confirm the successful formation of a ZnO/SiO_2 nanocomposite composed of crystalline ZnO nanoparticles supported on an amorphous silica matrix. The ZnO crystallites are in the nanometer range, well-dispersed yet partially agglomerated into micro-scale clusters, offering hierarchical porosity and extensive interfacial contact

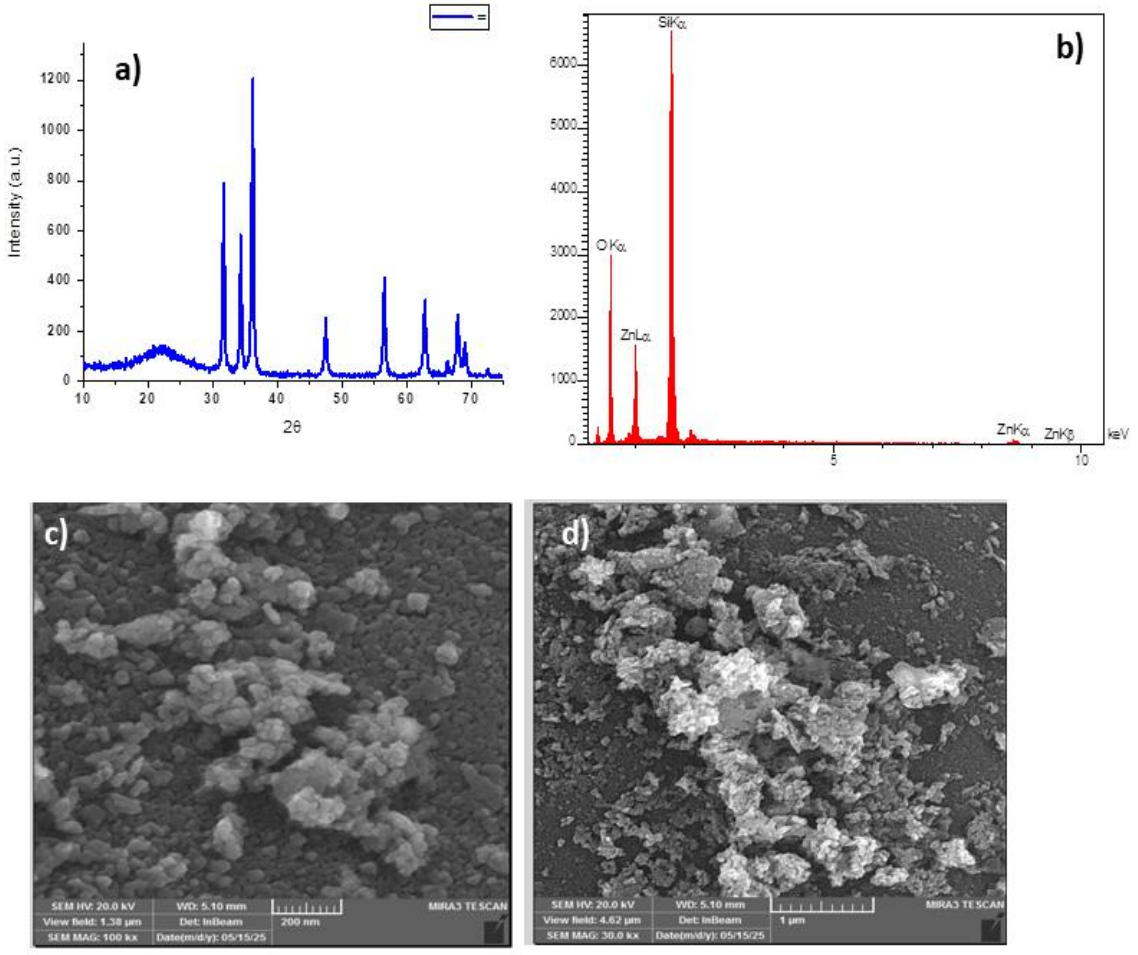

Fig. 2. Structural, compositional, and morphological characterization of ZnO/SiO_2 nanocomposite: (a) XRD pattern, (b) EDX spectrum, (c,d) SEM micrographs at 200 nm and 1 µm scales.

beneficial for functional applications.

Effect of loaded mass of SiO_2 / ZnO nanocomposite on photo catalytic degradation of the Congo red dye

The effect of the loaded mass of the SiO_2/ZnO nanocomposite on the photocatalytic degradation of Congo red dye was investigated under the following conditions: a dye concentration of 10 mg/L, an air flow rate of 10 mL/min, and ambient room temperature. As shown in Fig. 3, increasing the nanocomposite mass up to 0.15 g/100 mL led to a gradual enhancement in photocatalytic degradation efficiency. However, beyond this optimal value, the degradation efficiency began to decline [20].

At the optimal loading of 0.15 g/100 mL, the photocatalyst achieves maximum light absorption, enabling efficient generation of reactive species. However, when the mass exceeds this threshold, excess catalyst can cause light scattering and shielding effects. As a result, the penetration of UV light into deeper layers of the suspension is hindered, reducing the effective photocatalytic surface area and thus lowering degradation efficiency. This phenomenon has been reported

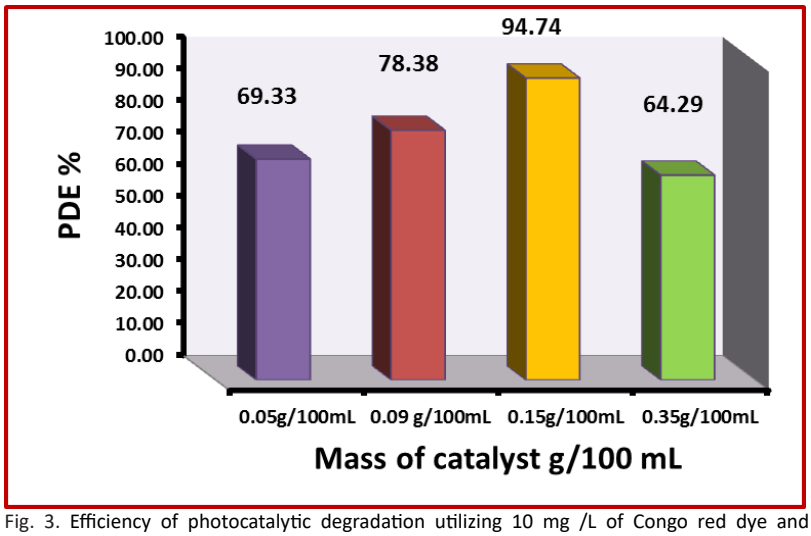

Fig. 3. Efficiency of photocatalytic degradation utilizing 10 mg /L of Congo red dye and 0.15g/100 mL SiO_2/ZnO nanocomposite.

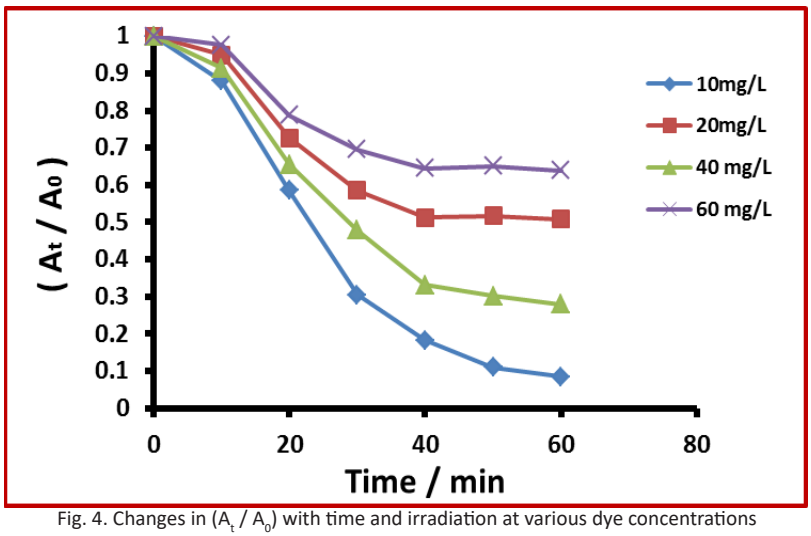

Fig. 4. Changes in (A_t / A_0) with time and irradiation at various dye concentrations

in several studies. Conversely, when the nanocomposite loading is below the optimal value, the photocatalytic efficiency also decreases. This reduction is attributed to the limited surface area of the catalyst available for light absorption and interaction with dye molecules, resulting in a lower rate of photo degradation [21, 22].

Effect initial concentration of Congo red dye on the photocatalytic

The effect of initial Congo red dye concentration on photocatalytic degradation was examined under constant experimental conditions, with dye concentrations ranging from 10 to 60 mg/L. The results are illustrated in Fig. 4. The data indicate that increasing the initial dye concentration leads to a reduction in the photocatalytic degradation rate. At lower dye concentrations, the solution is more transparent, allowing a greater number of photons to penetrate and reach the surface of the SiO_2/ZnO nanocomposite catalyst. This increased photon availability enhances the generation of reactive species such as hydroxyl radicals (•OH) and superoxide ions ($O_2•^-$), thereby accelerating the degradation of dye molecules. In contrast, at higher dye concentrations, the solution absorbs more light, reducing photon penetration and limiting catalyst activation, which ultimately suppresses degradation efficiency [23, 24].

When Congo red dye concentration was sufficient, the high photo degradation efficiency (91.45%) was (10 mg/L). Fig. 5 depicts the photocatalytic degradation efficiency (P.D.E.), which was determined at various Congo red dye concentrations.

Effect of initial pH on the photocatalytic degradation process

A series of experiments was conducted to evaluate the effect of initial pH on the photocatalytic degradation efficiency of Congo red dye, with pH values ranging from 4 to 9. These variations in pH were intended to elucidate the relationship between the surface charge of the SiO_2/ZnO nanocomposite and the ionic nature of the dye molecules. The pH was adjusted using 0.01 mol/L solutions of hydrochloric acid (HCl) and sodium hydroxide (NaOH). All experiments were carried out under identical conditions: 0.15 g/100 mL of the SiO_2/ZnO nanocomposite, 10 mg/L of Congo red dye, and an air flow rate of 10 mL/min at room temperature.

As illustrated in Figs. 6 and 7, the photocatalytic degradation rate was lowest in highly acidic conditions, with a removal efficiency of 69.33% at pH 4. The highest degradation efficiency was observed at pH 8, reaching 92.11%. In contrast, under basic conditions, the removal efficiency decreased to 60.16%. This variation in degradation performance across different pH levels can be attributed to the influence of pH on the surface charge of the catalyst, which in turn affects the

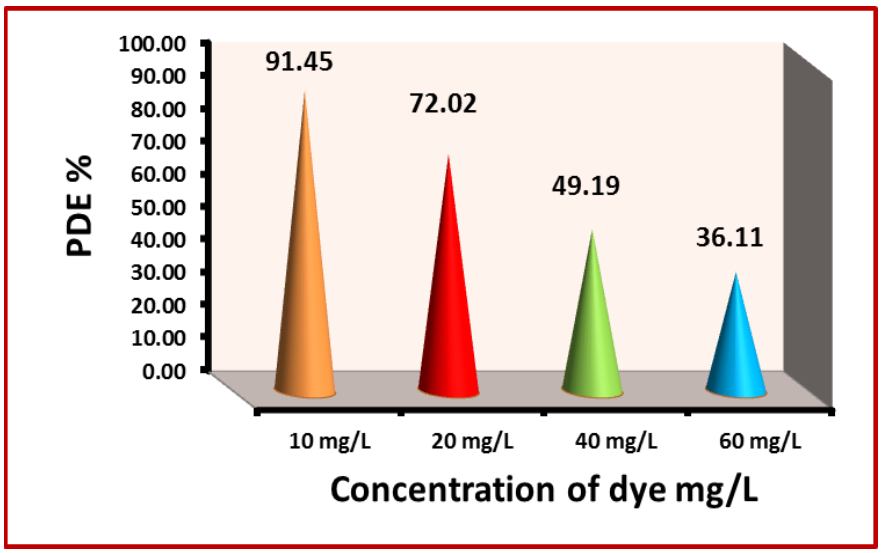

Fig. 5. Efficiency of photocatalytic degradation utilizing 10 ppm of Congo red dye and 0.15g/100 mL SiO_2/ZnO nanocomposite.

interaction between the dye molecules and the active sites on the photocatalyst surface [25, 26]

Effect of addition of H_2O_2 on the photocatalytic degradation process

The effect of hydrogen peroxide (H_2O_2) addition on the photocatalytic degradation of Congo red dye was studied over a concentration range of 0.098 mol·L^{-1} to 0.932 mol·L^{-1}. The results, presented in Fig. 8, demonstrate that the photocatalytic degradation efficiency initially increases with increasing H_2O_2 concentration, reaching an optimal value at 0.293 mol·L^{-1}. Beyond this concentration, however, a further increase in H_2O_2 leads to a decline in the degradation rate constant [27].

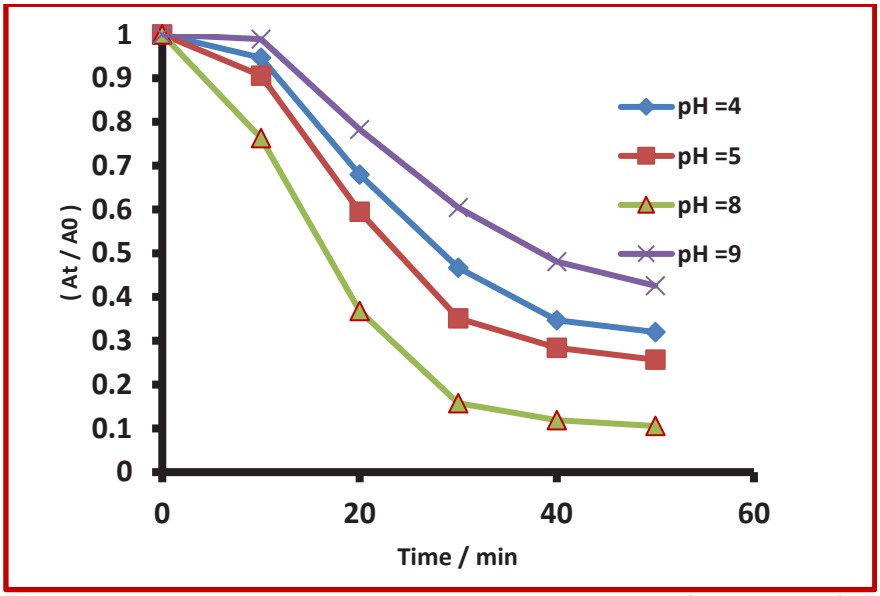

Fig. 6. Effect of pH on photocatalytic degradation of Congo red dye by 0.15 mg/ mL dose of SiO_2/ZnO nanocomposite with 10 mg/L.

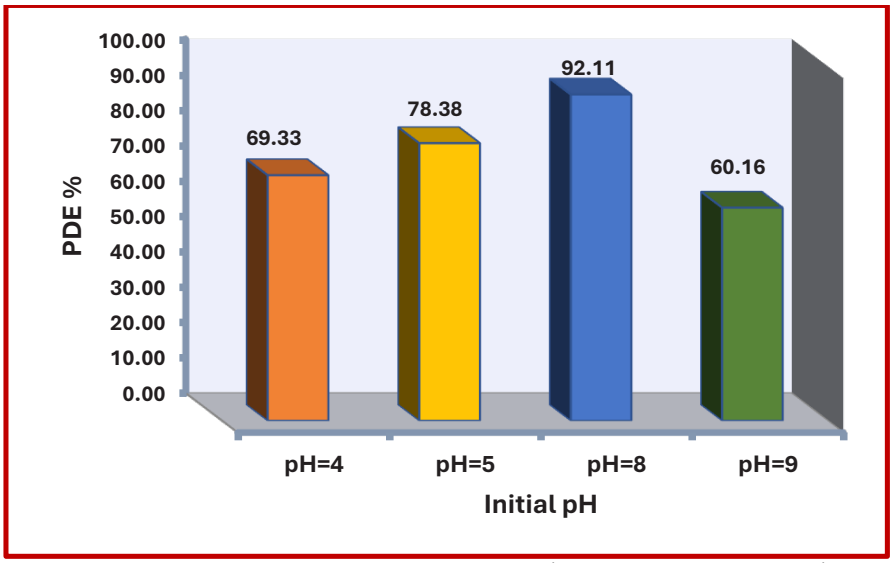

Fig. 7. Efficiency of photocatalytic degradation utilizing 10 mg/L of Congo red dye and 0.15g/100 mL SiO_2/ZnO nanocomposite with different pH.

The observed enhancement in degradation efficiency at lower H_2O_2 concentrations can be attributed to the increased generation of hydroxyl radicals (•OH), which are powerful oxidizing agents responsible for breaking down dye molecules. The following reaction illustrates the formation of hydroxyl radicals upon interaction between H_2O_2 and photogenerated electrons [28]:

$$SiO_2 (e^-) + H_2O_2 \rightarrow SiO_2 + OH^- + \bullet OH \quad (1)$$

H_2O_2 also reacts with superoxide anion to form • OH radical:

$$H_2O_2 + {}^{\bullet-}O_2 \rightarrow {}^{\bullet}OH + OH^- + O_2 \quad (2)$$

At higher concentrations, excess H_2O_2 may act as a scavenger of hydroxyl radicals or photogenerated holes, reducing the availability of these reactive species for dye degradation and thus diminishing overall efficiency, as shown in Eqs. 3 and 4:

$$H_2O_2 + {}^{\bullet}OH \rightarrow HO^{\bullet}_2 + H_2O \quad (3)$$

$$HO^{\bullet}_2 + {}^{\bullet}OH \rightarrow H_2O + O_2 \quad (4)$$

The Effect of Light Intensity on Photo degradation of Congo red dye

A series of experiments was performed to evaluate the effect of light intensity on the photocatalytic degradation of Congo red dye using the SiO_2/ZnO nanocomposite. The light

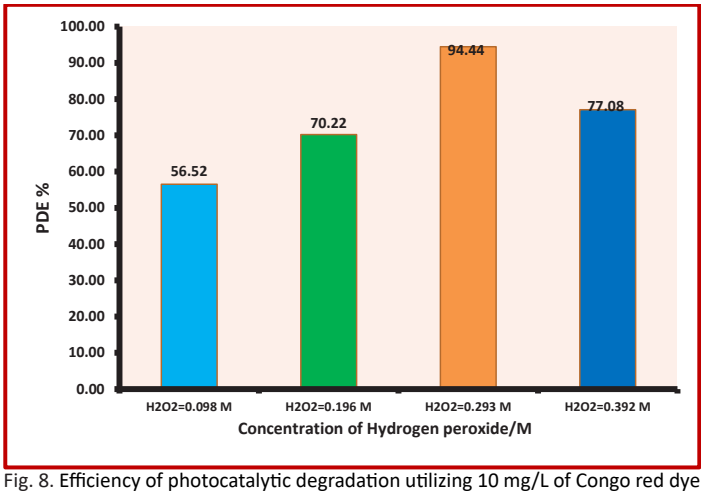

Fig. 8. Efficiency of photocatalytic degradation utilizing 10 mg/L of Congo red dye and 0.15g/100 mL SiO_2/ZnO nanocomposite with different H_2O_2 concentration.

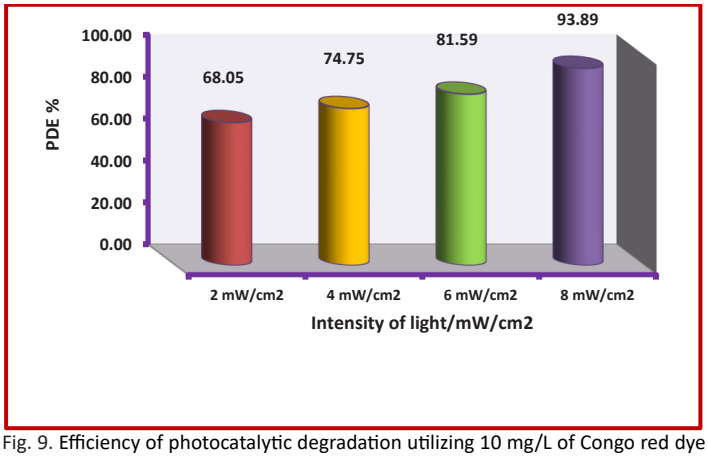

Fig. 9. Efficiency of photocatalytic degradation utilizing 10 mg/L of Congo red dye and 0.15g/100 mL SiO_2/ZnO nanocomposite with light intensity.

intensity was varied in the range of 2 to 8 mW/cm², while keeping other conditions constant: a dye concentration of 10 mg/L, a catalyst dosage of 0.15 g/100 mL, an air flow rate of 10 mL/min, and ambient room temperature. As shown in Fig. 9, an increase in light intensity resulted in a corresponding enhancement in the photocatalytic degradation rate of Congo red. This improvement can be attributed to the increased generation of photons, which promotes the excitation of electrons from the valence band (VB) to the conduction band (CB) of the photocatalyst, thereby producing more electron–hole pairs. These charge carriers are essential for initiating redox reactions that lead to the formation of reactive oxygen species (ROS), which are responsible for the degradation of dye molecules [29, 30].

Effect of temperature on photocatalytic degradation of Congo red dye

A series of experiments was conducted to investigate the influence of temperature on the photocatalytic degradation of Congo red dye within the temperature range of 293–308 K. The tests were carried out under constant conditions: an initial dye concentration of 10 mg/L, a SiO_2/ZnO nanocomposite catalyst dosage of 0.15 g/100 mL, and identical experimental settings across all trials. As illustrated in Fig. 10, the degradation rate of Congo red dye increased significantly with rising temperature. This enhancement in photocatalytic efficiency at elevated temperatures can be attributed to the increased generation of reactive hydroxyl radicals (•OH), which are key oxidizing agents in the degradation process.

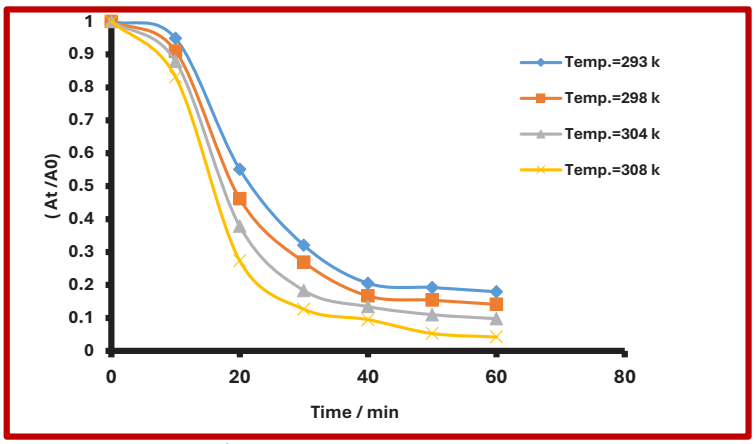

Fig. 10. The variation (A_t / A_0) with UV radiation exposure time and temperature, with initial Congo red dye concentrations of 10 mg/L and photocatalyst amounts of 0.15 g/100 ml.

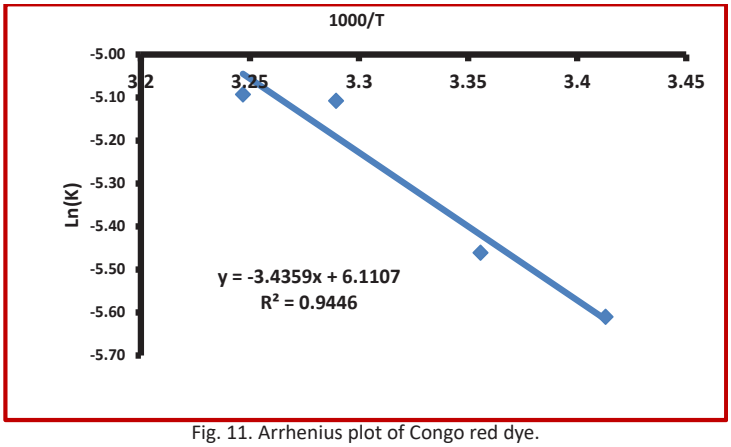

Fig. 11. Arrhenius plot of Congo red dye.

Additionally, higher temperatures may improve the mobility of reactant molecules and the rate of electron–hole separation, further facilitating the degradation reaction. As shown in Fig. 11, the apparent activation energy for the photocatalytic degradation process was determined by plotting ln k versus 1/T, following the Arrhenius equation. The calculated activation energy was found to be 38.61 kJ·mol^{-1}, indicating a thermally assisted photocatalytic process [31].

To evaluate the thermodynamic parameters associated with the photocatalytic degradation process, such as the enthalpy of activation (ΔH°) and entropy of activation (ΔS°), a linear relationship was obtained using the Eyring equation, as illustrated in Fig. 12.

$$ln\left(\frac{k}{T}\right) = -\left(\frac{\Delta H}{R} * \frac{1}{T}\right) + ln\left(\frac{K_B}{h}\right) + \frac{\Delta S}{R} \quad (5)$$

Where, KB= Boltzmann's constant (1.381×10^{-23}J\K), T= absolute temperature in Kelvin (K), h= plank constant (6.626×10^{-34} J•s), k: the rate constant.

According to the equation 5. a plot of ln(k\T) versus 1\T produces a straight line and the value of Enthalpy of activation can be calculated from the slop of this line (ΔH°=31.06 kJ\mol). And from the y-intercept the Entropy of activation value (ΔS°= -0.14842 k J\ mol. k). The positive value of Enthalpy of activation refers to endothermic reaction. In the present case the value of Entropy of activation is negative as in Table 1, so that the product formed is more ordered than the reactants.

$$\Delta G = \Delta H - T\Delta S \quad (6)$$

ΔG: Change in Gibbs free energy, ΔH: Change in Enthalpy, ΔS: Change in Entropy, T: absolute temperature in Kelvin (K).

The Gibbs' free energy ΔG° can be determined by utilizing the following formula: Eq. 6 and equal (44.19 kJ\mol). The positive values of ΔG° for the reaction suggest that the photocatalytic breakdown of the substance is not spontaneous for Congo red dye.

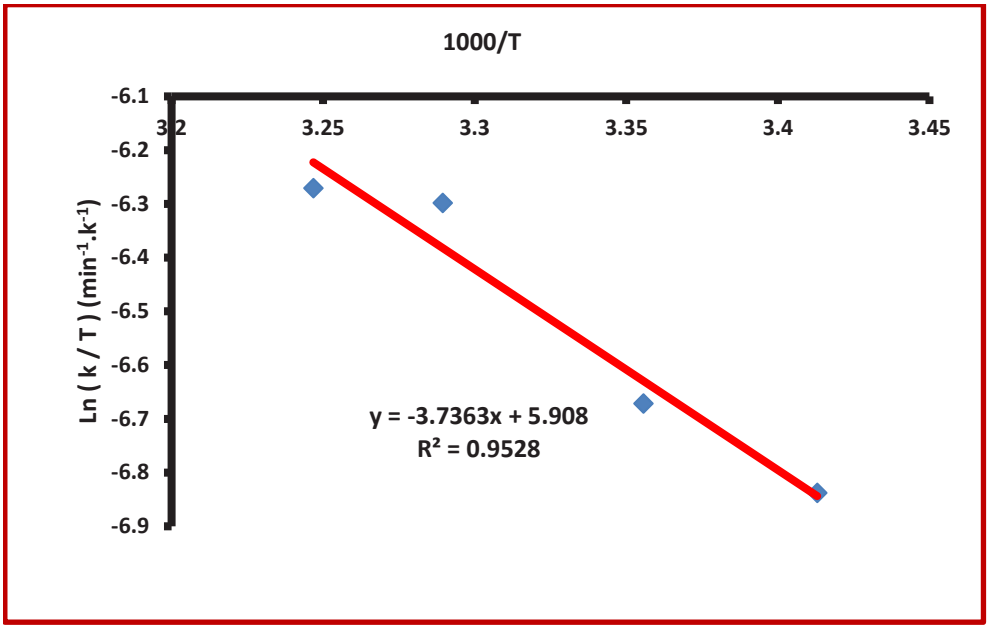

Fig. 12. Erying equation plot ln(k\T) against 1000\T for Congo red dye.

Table 1. The thermodynamic parameters of the photocatalytic degradation of dye.

Temperature/K	Enthalpy of activation/kJ · mol^{-1}	Entropy of activation/ KJ.mol^{-1}.k^{-1}	Gibbs' free energy/ kJ.mol^{-1}
298	31.06 KJ/mole	- 0.14842	44.19

Kinetics Studies

A series of experiments have been performed to estimate the kinetic model; the data was evaluated via pseudo-first-order reaction, which the following equation can describe

$$ln\left(\frac{A_o}{A_t}\right) = kt \quad (7)$$

and the data was evaluated via pseudo-second-order reaction which can be described by the following equation :

$$\frac{1}{[A]_t} - \frac{1}{[A]_o} = kt \quad (8)$$

The equation first model assumes that the solute uptake rate is directly proportional to the saturation concentration— the uptake quantity of dye through time. Plotting the natural logarithm

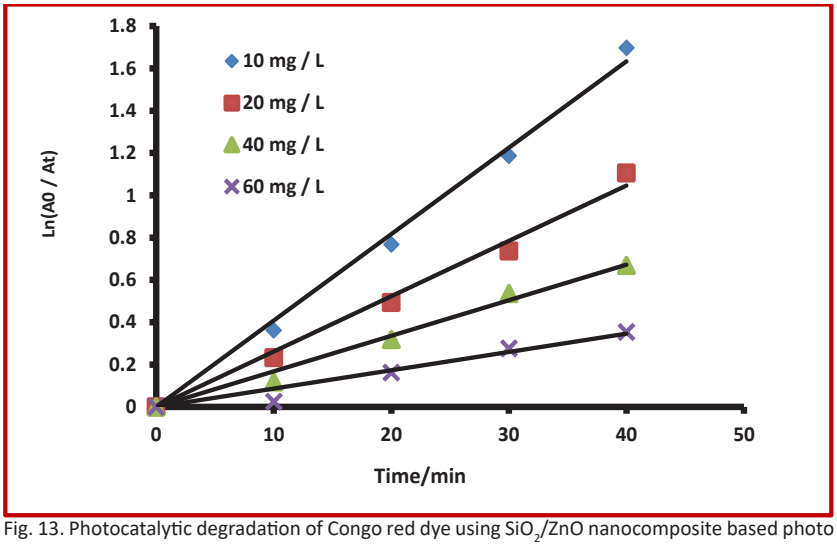

Fig. 13. Photocatalytic degradation of Congo red dye using SiO_2/ZnO nanocomposite based photo catalysts – first order reaction kinetics at different concentration of dye.

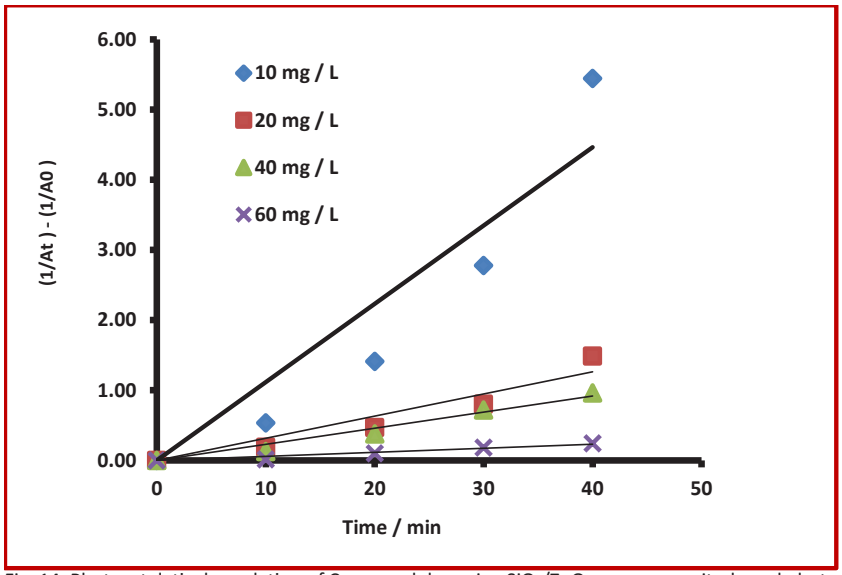

Fig. 14. Photocatalytic degradation of Congo red dye using SiO_2/ZnO nanocomposite-based photo catalysts – Second order reaction kinetics at different concentrations of dye.

of the ratio between the original concentration of Congo red dye and the concentration after photocatalytic degradation ($Ln(A_0/A_t)$ versus the corresponding irradiation time (min) yields a linear relationship as shown in Fig. 13. From the Fig. 14 the investigational result was flawlessly fitting to the kinetic model First order, by great values R_2 = 0.9963 at optimum dye concentration (10 mg/L).

The Table 2, Fig. 13 and Fig. 14 give the comparative kinetic parameters and the corresponding coefficients of determination for the Congo red dye photo degradation reaction using silica oxide nanoparticle. It is observed that silica oxide nanoparticle degraded Congo red dye according to first order kinetics [32].

Proposed Mechanism of photo catalysis of Congo red dye

When aqueous Congo red dyes solution was irradiated with UV radiation in the presence of SiO_2/ZnO nanocomposite electron promotes from valence band to conduction band of the silica oxide leaving behind a positive hole(h^+) in valence band as shown in Fig. 15. The photo electrons come into contact with oxygen, they will interact and produce superoxide radical anions ($^{\bullet-}O_2$). Furthermore, the vacancies in the valence band of the n-type ZnO will undergo a reaction with OH^- or H_2O, resulting in the formation of reactive oxygen species ($^{\bullet}OH$). Subsequently, the hydroxyl radical ($\bullet OH$) and superoxide radical ($\bullet O_2$) might

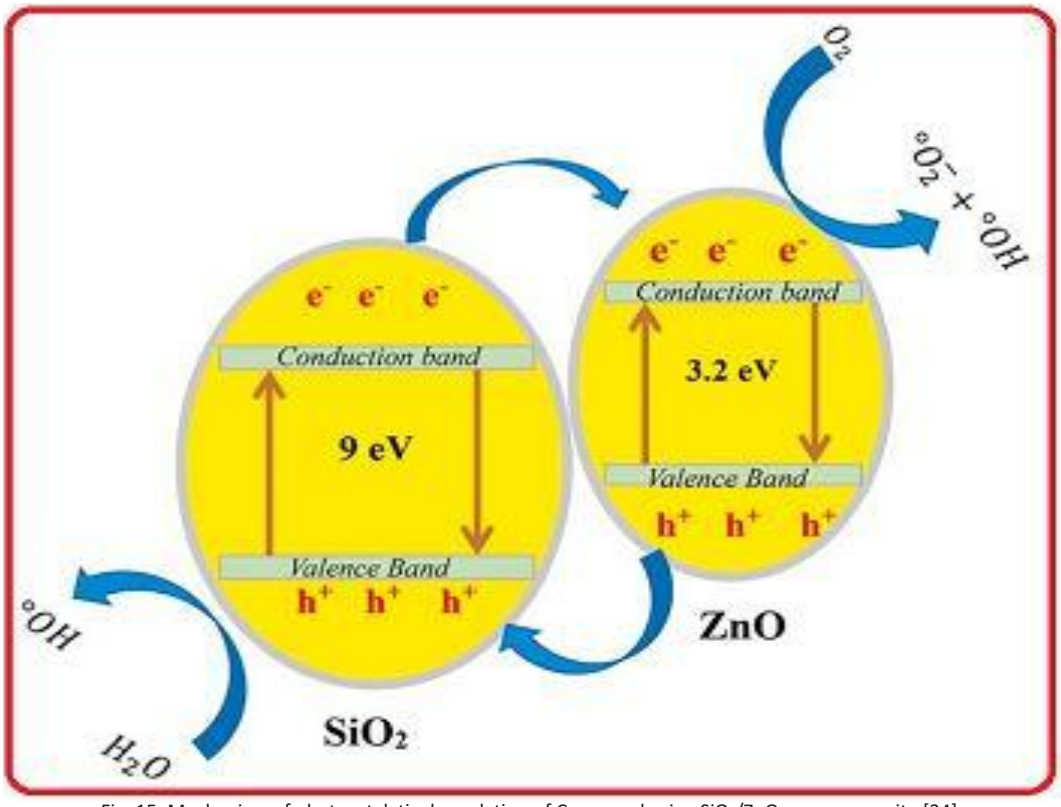

Fig. 15. Mechanism of photocatalytic degradation of Congo red using SiO_2/ZnO nanocomposite [34].

Table 2. Kinetic parameters for the photocatalytic degradation process of Congo red dye using SiO_2/ZnO nanocomposite as a catalyst.

Sample name	Concentration of Congo red dye(mg/L)	Pseudo-First order Kinetic model		Pseudo-Second order Kinetic model	
		K_1(min^{-1})	R^2	K_2(M. min^{-1})	R^2
SiO_2/ZnO nanocomposite	10	0.0408	0.9944	0.1116	0.8787
	20	0.0262	0.9899	0.0316	0.917
	40	0.0168	0.9875	0.0229	0.9692
	60	0.0087	0.9552	0.0058	0.9476

undergo a reaction with Congo red dye, resulting in its breakdown to H_2O and CO_2 is expected [33].

CONCLUSION

This work included synthesis of ZnO.SiO_2, the combined XRD, EDX, and SEM results confirm the successful formation of a ZnO/SiO_2 nanocomposite composed of crystalline ZnO nanoparticles supported on an amorphous silica matrix. Congo red dye photocatalytic degradation processes were dependent on the catalyst dosage, with 0.15 g of SiO_2/ZnO nanocomposite per 100 mL being the ideal value. The ideal value of Congo red dye (10 mg/L) has been researched in terms of the impact of dye concentration. When the concentration of Congo red dye is increased, the photocatalytic degradation slows down because there is less OH- adsorbed on the catalyst surface. The photocatalytic breakdown of Congo red dye has an efficiency of 94.44 %. Calculations show that the activation energy is 38.61kJ.mol^{-1}using Arrhenius equation, Enthalpy of activation=31.06 KJ.mol^{-1}, Entropy of activation= -0.14842 KJ.mol^{-1}.k^{-1}, Gibbs free energy =44.19 kJ.mol^{-1}.

CONFLICT OF INTEREST

The authors declare that there is no conflict of interests regarding the publication of this manuscript.

REFERENCES

1. Kulal, 1. Kulal P, Krishnappa PB, Badalamoole V. Development of gum acacia based magnetic nanocomposite adsorbent for wastewater treatment. Polym Bull. 2021;79(11):9457-9484.
2. Shah SS, Ramos B, Teixeira ACSC. Adsorptive Removal of Methylene Blue Dye Using Biodegradable Superabsorbent Hydrogel Polymer Composite Incorporated with Activated Charcoal. Water. 2022;14(20):3313.
3. Zhou Z, Lin S, Yue T, Lee T-C. Adsorption of food dyes from aqueous solution by glutaraldehyde cross-linked magnetic chitosan nanoparticles. J Food Eng. 2014;126:133-141.
4. Shen Y, Li B, Zhang Z. Super-efficient removal and adsorption mechanism of anionic dyes from water by magnetic amino acid-functionalized diatomite/yttrium alginate hybrid beads as an eco-friendly composite. Chemosphere. 2023;336:139233.
5. Thamer BM, Shaker AA, Abdul Hameed MM, Al-Enizi AM. Highly selective and reusable nanoadsorbent based on expansive clay-incorporated polymeric nanofibers for cationic dye adsorption in single and binary systems. Journal of Water Process Engineering. 2023;54:103918.
6. Maryudi M, Amelia S, Salamah S. Removal of Methylene Blue of Textile Industry Waste with Activated Carbon using Adsorption Method. Reaktor. 2019;19(4):168-171.
7. Paliwal G, Ameta N, Tak P. Photocatalytic degradation of fast green dye using green synthesized nickel oxide nanoparticles. Research Journal of Chemistry and Environment. 2025;12(29):23.
8. Aljeboree AM, Al-Baitai AY, Abdalhadi SM, Alkaim AF. Investigation Study of Removing Methyl Violet Dye From Aqueous Solutions Using Corn-Cob as A Source of Activated Carbon. Egyptian Journal of Chemistry. 2021;0(0):0-0.
9. Boudechiche N, Fares M, Ouyahia S, Yazid H, Trari M, Sadaoui Z. Comparative study on removal of two basic dyes in aqueous medium by adsorption using activated carbon from Ziziphus lotus stones. Microchem J. 2019;146:1010-1018.
10. Aljeboree AM, Alkaim AF. Removal of Antibiotic Tetracycline (TCs) from aqueous solutions by using Titanium dioxide (TiO_2) nanoparticles as an alternative material. Journal of Physics: Conference Series. 2019;1294(5):052059.
11. Yasin G, Jasim SA, Raya I, Kzar HH, Abed Hussein B, Al-Gazally ME, et al. Computational Study of Interaction and Removal of Benzopyran by Anatase Titanium Dioxide Nanoparticle. Polycyclic Aromatic Compounds. 2022;43(5):4467-4477.
12. Aljeboree AM, Hussein SA, Jawad MA, Alkaim AF. Hydrothermal synthesis of eco-friendly ZnO/CNT nanocomposite and efficient removal of Brilliant Green cationic dye. Results in Chemistry. 2024;7:101364.
13. Bessaha G, Bessaha F, Mahrez N, Boucif F, Çoruh A, Khelifa A. Enhancement of the comprehensive performance of tetracycline adsorption by halloysite nanotubes: Kinetics, mechanism, and reusability study. Desalination and Water Treatment. 2024;320:100695.
14. Borah M, Konwar U, Gogoi P, Boruah P, Bora JG, Garg S, et al. Decolorization of tea industry wastewater utilizing tea waste bio-adsorbent in fixed-bed adsorption column: breakthrough curves analysis and modeling. Sustainable Water Resources Management. 2024;10(1).
15. Bessaha F, Mahrez N, Marouf-Khelifa K, Çoruh A, Khelifa A. Removal of Congo red by thermally and chemically modified halloysite: equilibrium, FTIR spectroscopy, and mechanism studies. Int J Environ Sci Technol (Tehran). 2018;16(8):4253-4260.
16. Seyahmazegi EN, Mohammad-Rezaei R, Razmi H. Multiwall carbon nanotubes decorated on calcined eggshell waste as a novel nano-sorbent: Application for anionic dye Congo red removal. Chem Eng Res Des. 2016;109:824-834.
17. Syahnur FR, Permana MD, Pratama RA, Deawati Y, Lutfi Firdaus M, Rakhmawaty Eddy D, et al. Exploring chemical, physical, and biosynthesis methods for ZnO/SiO_2: Synthesis strategies and applications. Inorg Chem Commun. 2025;171:113659.
18. Ghattavi S, Homaei A. Synthesis and characterization of ZnO-SiO_2 hybrid nanoparticles as an effective inhibitor for marine biofilm and biofouling. J Mol Liq. 2024;396:123974.
19. Luo Z, Lu J, Yan Q, Hu D, Zhou Y. Influence of SiO_2–ZnO mixed soft abrasive on tribological behavior and polishing performance of sapphire wafer. Mater Sci Semicond Process. 2024;176:108318.
20. Karthik KV, Raghu AV, Reddy KR, Ravishankar R, Sangeeta M, Shetti NP, et al. Green synthesis of Cu-doped ZnO nanoparticles and its application for the photocatalytic degradation of hazardous organic pollutants. Chemosphere. 2022;287:132081.
21. Insuwan W, Rangsriwatananon K. Removal of Paraquat from Aqueous Solutions onto Zeolite LTL. Eng J. 2017;21(2):15-23.
22. Subhi HM, Bader AT, Al-Gubury HY. Synthesis and

Characterization of ZnO Nanoparticles via Thermal Decomposition for Zn(II) Schiff Base Complex. Indonesian Journal of Chemistry. 2022;22(5):1396.
23. Shubha JP, Kavalli K, Adil SF, Assal ME, Hatshan MR, Dubasi N. Facile green synthesis of semiconductive ZnO nanoparticles for photocatalytic degradation of dyes from the textile industry: A kinetic approach. Journal of King Saud University - Science. 2022;34(5):102047.
24. Efficient Adsorption and Removal of the Herbicide 2,4-Dichlorophenylacetic Acid from Aqueous Solutions Using MIL-88(Fe)-NH2. American Chemical Society (ACS).
25. Shalinibabu C, Nagaraja KK, Pramodini S. Improved adsorption and photocatalytic degradation of acid Blue 25 dye using pristine and Al doped zinc oxide. Inorg Chem Commun. 2025;177:114413.
26. Photocatalytic Degradation of Industrial Dye Wastewater Using Zinc Oxide-Polyvinylpyrrolidone Nanoparticles. Malaysian Journal of Analytical Science. 2018;22(4).
27. Sukkasem T, Nuchitprasittichai A, Junpirom S, Pulsawat N, Khumronrith P, Photongngam S, et al. Role of SiO_2 in TiO2/SiO_2 photocatalyst for hydrogen peroxide gas generation from air humidity via photocatalysis. J Incl Phenom Macrocycl Chem. 2023;104(5-6):289-305.
28. Junpirom S, Sukkasem T, Nuchitprasittichai A, Janphuang P. TiO_2/SiO_2 Coated 310S Stainless Steel for Hydrogen Peroxide Generation via Photocatalytic Reaction. Current Applied Science and Technology. 2021;22(3).
29. Regalado-Raya R, Romero-Romero R, Avilés-García O, Espino-Valencia J. Synthesis and Characterization of TiO_2/SiO_2 Monoliths as Photocatalysts on Methanol Oxidation. International Journal of Photoenergy. 2018;2018:1-8.
30. Manzoor U, Islam M, Tabassam L, Rahman SU. Quantum confinement effect in ZnO nanoparticles synthesized by co-precipitate method. Physica E: Low-dimensional Systems and Nanostructures. 2009;41(9):1669-1672.
31. Zak AK, Abrishami ME, Majid WHA, Yousefi R, Hosseini SM. Effects of annealing temperature on some structural and optical properties of ZnO nanoparticles prepared by a modified sol–gel combustion method. Ceram Int. 2011;37(1):393-398.
32. Insight into the Influence of ZnO Defectivity on the Catalytic Generation of Environmentally Persistent Free Radicals in ZnO/SiO_2 Systems. American Chemical Society (ACS).
33. Fatimah I, Fadillah G, Sahroni I, Kamari A, Sagadevan S, Doong R-A. Nanoflower-like composites of ZnO/SiO_2 synthesized using bamboo leaves ash as reusable photocatalyst. Arabian Journal of Chemistry. 2021;14(3):102973.
34. Arghavan FS, Al-Musawi TJ, Allahyari E, Moslehi MH, Nasseh N, Hossein Panahi A. Complete degradation of tamoxifen using $FeNi_3$@SiO_2@ZnO as a photocatalyst with UV light irradiation: A study on the degradation process and sensitivity analysis using ANN tool. Mater Sci Semicond Process. 2021;128:105725.